International Journal of Pharmaceutics 403 (2011) 170–177

Contents lists available at ScienceDirect

International Journal of Pharmaceutics

journal homepage: www.elsevier.com/locate/ijpharm

Pharmaceutical Nanotechnology

# PET imaging of brain cancer with positron emitter-labeled liposomes

Naoto Oku[a,*], Mina Yamashita[a], Yurie Katayama[a], Takeo Urakami[a,1], Kentaro Hatanaka[a], Kosuke Shimizu[a], Tomohiro Asai[a], Hideo Tsukada[b], Shuji Akai[c], Hiroaki Kanazawa[d]

[a] Department of Medical Biochemistry and Global COE, Graduate School of Pharmaceutical Sciences, University of Shizuoka, Yada, Suruga-ku, Shizuoka 422-8526, Japan
[b] PETCenter, Central Research Laboratory, Hamamatsu Photonics K.K. Hirakuchi, Hamakita-ku, Hamamatu, Shizuoka 434-8601, Japan
[c] Department of Synthetic Organic Chemistry, Graduate School of Pharmaceutical Sciences, University of Shizuoka, Yada, Suruga-ku, Shizuoka 422-8526, Japan
[d] Department of Anatomy, School of Nursing, University of Shizuoka, Yada, Suruga-ku, Shizuoka 422-8526, Japan

ARTICLE INFO

*Article history:*
Received 6 May 2010
Received in revised form
30 September 2010
Accepted 2 October 2010
Available online 8 October 2010

*Keywords:*
Positron emission tomography
Brain cancer
Liposome
Cancer diagnosis
Passive targeting
Angiogenesis

ABSTRACT

Since nanocarriers such as liposomes are known to accumulate in tumors of tumor-bearing animals, and those that have entrapped a positron emitter can be used to image a tumor by PET, we applied $^{18}$F-labeled 100-nm-sized liposomes for the imaging of brain tumors. Polyethylene glycol (PEG)-modified liposomes, which are known to accumulate in tumors by passive targeting and those modified with Ala-Pro-Arg-Pro-Gly, which are known to home into angiogenic sites were used. Those liposomes labeled with DiI fluorescence accumulated in a glioma implanted in a rat brain 1 h after the injection, although they did not accumulate in the normal brain tissues due to the protection afforded by the blood–brain barrier. Preformed liposomes were easily labeled with 1-[$^{18}$F]fluoro-3,6-dioxatetracosane, and enabled the imaging of gliomas by PET with higher contrast than that obtained with [$^{18}$F]deoxyfluoroglucose. In addition, the smallest tumor among those tested, having a diameter of 1 mm was successfully imaged by the liposomal $^{18}$F. Therefore, nanocarrier-based imaging of brain tumors is promising for the diagnosis of brain cancer and possible drug delivery-based therapy.



## 1. Introduction

Brain cancers such as glioblastomas are known to be aggressive and invasive (Wen and Kesari, 2008). Therefore, diagnosis of brain cancer at the early stages is quite important. Positron emission tomography (PET) is one of the strong tools for diagnosis, therapeutic evaluation, and prognostic evaluation of cancer. [2-$^{18}$F]-2-deoxyfluoro-D-glucose (FDG) is the most widely used positron emitter for cancer diagnosis (Scott et al., 2008; Nakamoto et al., 2009). However, the utility of FDG-PET imaging for detection of brain cancer is controversial due to the high demand for glucose in the brain (Takeda et al., 2003; Chen, 2007). To reduce this bothersome background various compounds such as [$^{11}$C]choline (Tian et al., 2004; Kato et al., 2008), [$^{11}$C]acetate (Yamamoto et al., 2008), and amino acid analogues such as [$^{11}$C]methionine (Hatakeyama et al., 2008; Jager et al., 2001), L-[methyl-$^{11}$C]methionine (Nojiri et al., 2009; Ullrich et al., 2009), *O*-[$^{11}$C]methyl-L-tyrosine (Ishiwata et al., 2004), *O*-[$^{18}$F]fluoromethyl-L-tyrosine (Ishiwata et al., 2004), *O*-[$^{18}$F]fluoroethyl-L-tyrosine (Heiss et al., 1999; Langen et al., 2006; Floeth et al., 2007; Mehrkens et al., 2008; Pauleit et al., 2009), and *O*-[$^{18}$F]fluoropropyl-L-tyrosine (Tang et al., 2003) have been synthesized and evaluated as PET imaging agents for the diagnosis and detection of recurrence of brain tumors. Among them, the amino acid analogues show relatively low accumulation in normal peripheral tissue (low tissue-to-blood ratio) and rapid blood clearance and have been used for detecting brain tumors and other tumors as well. We also demonstrated that the D-amino acid analogue *O*-[$^{18}$F]fluoromethyl-D-tyrosine is useful for tumor imaging by PET (Urakami et al., 2009).

Nanomedicines such as liposomal drugs are known to accumulate in tumors due to the enhanced permeability of tumor blood vessels and the retention effect (Maeda et al., 2000, 2009). This drug delivery system (DDS) strategy is based on the nature of tumors: tumor cells demand oxygen and nutrition and cause angiogenesis for obtaining them, and angiogenic vessels are leaky enough to be permeated by nano-sized materials. Liposomes are known as one of the most effective drug carriers for cancer therapy. In liposomal DDS technologies, polyethylene glycol (PEG)-modified liposomes are useful drug carriers for cancer therapy; for they have a characteristically long circulation time in the bloodstream due to avoidance of being trapped by the reticuloendothelial system (RES) such as in the liver and spleen (Sakakibara et al., 1996;

* Corresponding author. Tel.: +81 54 264 5701; fax: +81 54 264 5705.
*E-mail address:* oku@u-shizuoka-ken.ac.jp (N. Oku).
[1] Present address: The Burnham Institute for Medical Research at Lake Nona, 6400 Sanger Rd., Orlando, FL 32827, United States.

0378-5173/$ – see front matter © 2010 Elsevier B.V. All rights reserved.
doi:10.1016/j.ijpharm.2010.10.001

Gabizon, 2001). PEG-modified liposomes tend to accumulate in tumor tissues through passive targeting, and PEG-modified liposomes containing doxorubicin have been used in clinical cancer therapy.

We previously demonstrated that PEG-liposomes encapsulating [$^{18}$F]FDG accumulate in solid tumors and can be effectively imaged by PET (Oku et al., 1996). Although the encapsulation efficiency of [$^{18}$F]FDG is not so high, the result indicated the usefulness of liposomes or nanocarriers for cancer imaging. Moreover, actively targeting nanocarriers specifically associating with tumor cells or angiogenic vessels are an attractive approach. For example, we previously demonstrated that liposomes modified with a peptide specifically recognized by membrane type-1 matrix metalloproteinase (MT1-MMP), which is expressed on the surface of angiogenic endothelial cells, accumulate in tumors (Kondo et al., 2004). In that study, we encapsulated [$^{18}$F]FDG in the liposomes and determined the distribution of the liposomes by PET. We also performed *in vivo* biopanning of a phage-displayed peptide library using an angiogenesis mouse model to obtain specific probes for angiogenic endothelial cells, and identified the Ala-Pro-Arg-Pro-Gly (APRPG) motif as a novel peptide homing to angiogenic vessels (Oku et al., 2002; Asai et al., 2002). Liposomes modified with APRPG and labeled with [$^{3}$H]cholesterol hexadecylether actually accumulate in tumors of colon 26 NL-17 carcinoma-implanted mice (Maeda et al., 2004). Moreover, the accumulation of APRPG-modified liposomes in such tumors was also confirmed by PET analysis using [$^{18}$F]FDG-encapsulated liposomes (Maeda et al., 2006).

In the present study, we applied PEG-modified and APRPG–PEG-modified liposomes entrapping a positron-emitter to brain tumor imaging by PET. At first, we analyzed distribution of fluorescence-labeled liposomes in glioma-bearing brain of rats by use of fluorescence microscopy and an *in vivo* fluorescence-based imaging system. Then PET imaging of brain cancers was achieved by use of 1-[$^{18}$F]fluoro-3,6-dioxatetracosane ([$^{18}$F]SteP2)-labeled liposomes. Our results indicate that even a 1-mm diameter brain tumor could be imaged by PET, thus demonstrating the usefulness of these liposomes for PET imaging of brain cancer.

## 2. Materials and methods

### 2.1. Preparation of liposomes

All lipids were the products of Nippon Fine Chemical, Co. Ltd. (Takasago, Hyogo, Japan). Distearoylphosphatidylcholine (DSPC) and cholesterol along with DSPE–PEG or DSPE–PEG–APRPG (10:5:1 as a molar ratio) were dissolved in chloroform/*t*-butanol to formulate PEG-modified liposomes (PEG-liposomes) or APRPG–PEG-modified liposomes (APRPG-liposomes), respectively. For fluorescence labeling of liposomes, 1,1′-dioctadecyl-3,3,3′,3′-tetramethyl-indocarbocyanine perchlorate (DiI, Molecular Probes Inc., Eugene, OR, USA) was added to the initial chloroform/*t*-butanol solution at a concentration of 1 mol% of DSPC. After the lipids had been dried under reduced pressure and stored *in vacuo* for at least 1 h, liposomes were prepared by hydration of the thin lipid film with 0.3 M glucose solution and frozen and thawed for 3 cycles by using liquid nitrogen. Then, the liposomes were sized by extruding them thrice through a polycarbonate membrane filter with 100-nm pores (Nuclepore track-Etch Membrane, Lipex). Particle size and $\zeta$-potential of PEG-liposomes and APRPG-liposomes were measured by use of a Zetasizer Nano ZS (MALVERN, Worcestershire UK, USA) and found to be 113 nm and −2.0 mV, respectively, for PEG-liposomes and 107 nm and −3.3 mV, respectively, for the APRPG-liposomes.

### 2.2. Preparation of brain cancer-bearing model rats

The glioma-bearing rat model was prepared by a modification of the procedure described previously (Takeda et al., 2003). Nine-week-old Fischer 344 male rats (Japan SLC, Hamamatsu, Japan) were cared for according to the Animal Facility Guidelines of the University of Shizuoka. For the implantation of tumor cells, the rats were anesthetized with chloral hydrate (40 mg/kg) in saline and individually placed in a stereotaxic apparatus. C6 glioma cells were maintained in Dulbecco's modified Eagle medium (DMEM, Wako Fine Chemical Co. Ltd., Osaka, Japan) supplemented with 10% heat-inactivated fetal bovine serum (Japan Bioserum Co. Ltd., Japan), penicillin G (100 U/mL) and streptomycin (100 μg/mL) at 37 °C in 5% $CO_2$ atmosphere. After harvesting of these cells, the cells were suspended in DMEM containing 1% gelatin ($2 \times 10^7$ cells/mL). Ten microliters of the cell suspension or vehicle (DMEM containing 1% gelatin) was injected at a rate of 0.7 μL/min into the left midbrain of each rat (4.3 mm posterior to bregma, 3.9 mm lateral to the midline suture, and 7.0 mm in depth) with an infusion pump (11 Plus, Harvard Apparatus, USA).

### 2.3. Intratumoral localization of DiI-labeled liposomes

C6 glioma cells ($2.0 \times 10^5$ cells/rat) were inoculated as described above. DiI-labeled liposomes were administered via a tail vein of the rat at 11 days after tumor implantation. One hour or 24 h after the injection of liposomes (0.5 mL/rat, 5 μmol as DSPC), the rats were anesthetized with chloral hydrate, perfused with *ca.* 200 mL saline and with *ca.* 100 mL 20% formaldehyde for the fixation. The brain was removed and sliced at a 2-mm thickness with a cryostat microtome (HM 505E, Microm, Walldorf, Germany). The slices were then incubated twice in PBS for 4 h each time at 4 °C, and then overnight in 30% sucrose solution at 4 °C. After removal of water, the slices were embedded in optimal cutting temperature compound (Sakura Finetech, Co. Ltd., Tokyo, Japan) and frozen at −80 °C. Brain sections (10 μm) were prepared with a cryostat microtome, and mounted on MAS-coated slides (Matsunami Glass Ind., Ltd., Japan) for observation with a fluorescence microscope (IMT-2, Olympus, Japan). Then, the slices were stained with hematoxylin and eosin (HE) and observed under the microscope.

### 2.4. Ex vivo imaging of the distribution of DiI-labeled liposomes

DiI-labeled liposomes (0.5 mL/rat, 5 μmol as DSPC) were administered via a tail vein of a rat at 9 days after the implantation of C6 glioma cells. One hour after the injection, the rats were sacrificed; and brain slices (2-mm thickness) were then prepared with a cryostat microtome without perfusion and fixation. Fluorescent images of those slices were obtained with a fluorescence imaging system (IVIS Lumina, Xenogen).

### 2.5. Preparation of positron emitter-labeled liposomes

Preparation of 1-[$^{18}$F]fluoro-3,6-dioxatetracosane (SteP2) and liposome labeling by the SophT method were performed as described previously (Urakami et al., 2007). About 100 MBq of [$^{18}$F]SteP2 in ethanol solution was transferred to a glass test tube, and the solvent was removed completely at 90 °C with a helium gas flow. Liposomal solution (1 mL, 10 μmol as DSPC) was added to the vial having a thin film of $^{18}$F-radiolabeled compound and incubated at 65 °C for 15 min with 5-s mixing by a vortex stirrer every 3 min. After the incubation, the liposomal solution was washed with PBS by centrifugation at 100,000 × *g* for 15 min (Beckman, Fullerton, CA, USA), and the pellet was resuspended and diluted in PBS to make a 22 MBq/mL solution. Radioactivity was measured with a curie meter (IGC-3, Aloka, Japan).

Rats anesthetized with chloral hydrate at 11 days after the implantation of C6 glioma cells were placed on an animal CT (Clairvivo CT, Shimadzu, Japan) to obtain CT images. Then, [$^{18}$F]SteP2-labeled liposomes (10 MBq/rat) were administered via a tail vein. PET scans were started immediately after the injection and continued for 60 min by use of an animal PET apparatus (Clairvivo PET, Shimadzu, Japan).

FDG-PET was similarly performed. [$^{18}$F]FDG (10 MBq/rat) was injected into the rats after having obtained the CT images.

### 2.6. PET analysis and autoradiography

Before PET analysis, rats anesthetized with chloral hydrate at 11 days after the implantation of C6 glioma cells were placed on the animal CT to obtain CT images. Then, [$^{18}$F]SteP2-labeled liposomes (10 MBq/rat) were administered via a tail vein. Then the PET scan was started immediately after the injection and continued for 60 min. FDG-PET was similarly performed. [$^{18}$F]FDG (10 MBq/rat) was injected into the rats after having obtained the CT images.

After the PET scan, the rats were sacrificed; and the brain was then excised. Thereafter, 2-mm slices were prepared and set on an imaging plate. Autoradiograms were obtained by using a bioimaging analyzer system (BAS2000, Fuji Film, Japan).

### 2.7. Biodistribution of liposomes

Glioma-bearing rats were injected with [$^{18}$F]SteP2-labeled PEG-liposomes (10 MBq/rat) via a tail vein as described above. At 1 h after the injection, the rats were sacrificed, and blood and organs (heart, lung, liver, spleen kidney normal part of brain, brain tumor) were removed. The radioactivity of blood and each organ was measured by using an auto gamma counter (1480 Wizard 3, Perkin Elmer, USA).

### 2.8. Statistical analysis

Differences between groups were evaluated by analysis of variance (ANOVA) with the Tukey *post hoc* test.

## 3. Results

### 3.1. Intratumoral distribution of fluorescence-labeled PEG- and APRPG-liposomes

At first, we confirmed that the angiogenic vessels formed by experimental glioma in the rat brain were leaky enough to allow permeation by nanomedicines such as liposomes. As shown in Fig. 1B and E, the DiI fluorescence of DiI-labeled PEG-liposomes and APRPG-liposomes, respectively, was observed in the glioma at 1 h after intravenous injection of the liposomes. Since DiI fluorescence was not observed in the normal brain tissues near the tumor, we concluded that the liposomes had accumulated in the tumor through angiogenic vessels. The fluorescence intensity was increased at 24 h after the injection (Fig. 1C and F). Interestingly, the DiI fluorescence of the PEG-liposomes accumulated widely in the tumor, although that of APRPG-liposomes accumulated intensely in rather specific areas, suggesting that these liposomes had accumulated in the angiogenic vessels. These patterns of liposomal fluorescence are consistent with our previous data obtained by use of tumor-bearing mice that had been implanted subcutaneously with C26 NL-17 colon carcinoma (Maeda et al., 2006).

To understand the structure of the brain vasculature, we examined normal and glioma-implanted brain specimens after HE-staining. As shown in Fig. 2, capillaries in the normal brain tissue were covered with astrocytes (Fig. 2A); whereas capillaries in the brain tumor tissues were surrounded directly by glioma cells (Fig. 2B). These results support the idea that the blood–brain barrier (BBB) is immature in angiogenic vessels of brain tumors. The possible architecture based on our observation and the literature (Standring, 2005) is shown in Fig. 2C and D.

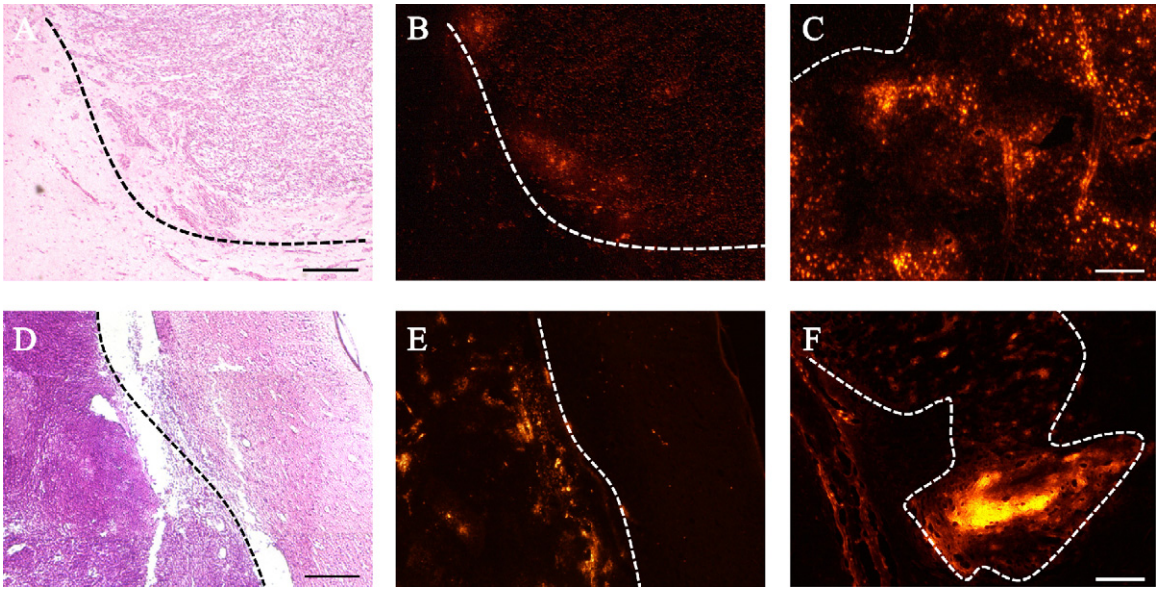


**Fig. 1.** Intratumoral distribution of fluorescence-labeled liposomes in brain tumor after intravenous injection. Rats were intravenously injected with DiI-labeled PEG-liposomes (A–C) or APRPG-liposomes (D–F) at day 11 after implantation of C6 glioma cells into the left midbrain. At 1 h (A, B, D, and E) or 24 h (C and F) after the injection, the brain tumors were dissected; and 10-μm frozen sections were prepared as described in Section 2. Then, liposomal distribution in the brain was observed under a fluorescence microscope (B, C, E, and F). Red fluorescence shows the liposomal localization. A and D show the images stained with hematoxylin and eosin, corresponding to the fluorescent images of "B" and "E", respectively. The dotted lines show the borders between normal and tumor tissue. Deep purple regions in "A" and "D" indicate the tumor tissues. The scale bar represents 100 μm.

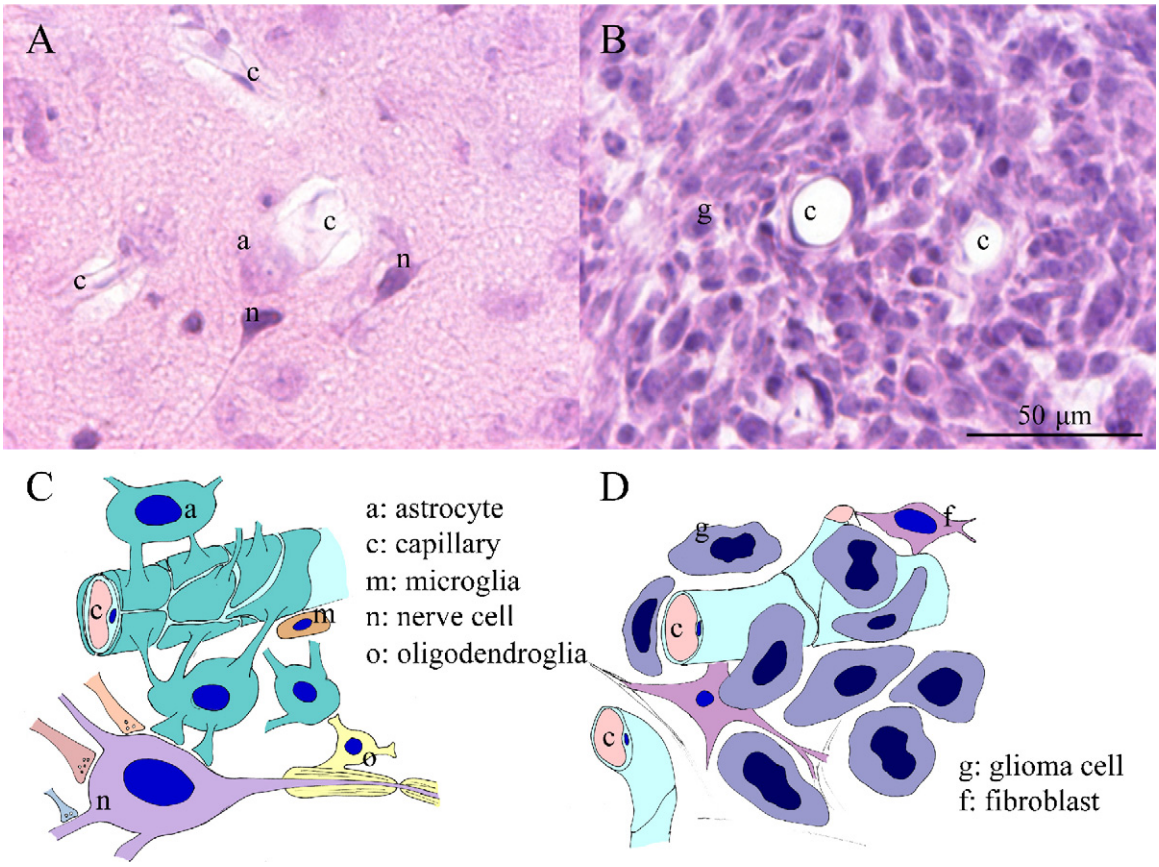


**Fig. 2.** Structure around blood capillaries in normal brain and brain tumor tissues. A rat brain tumor model was prepared by the implantation of C6 glioma cells into the left midbrain. The brain was dissected, and 10-μm sections of normal right brain (A) and tumor-implanted left brain (B) were stained with hematoxylin and eosin. Schematic interpretation of the histology around blood capillaries in normal brain (C) and brain tumor tissues (D) are shown.

### *3.2. Ex vivo study on the accumulation of fluorescence-labeled liposomes in brain tumor*

Although microscopic study provided data on the intratumoral distribution of the liposomes, the liposomal distribution in the whole brain could not be understood. Therefore, we next examined the distribution of DiI-labeled liposomes in the glioma-bearing brain by use of whole-brain slices. As a result, both PEG-liposomes and APRPG-liposomes accumulated in the brain tumor 1 h after the injection via a tail vein (Fig. 3B and D, respectively). No specific accumulation could be observed in the sham-operated brain after the injection of the DiI-labeled PEG-liposomes (Fig. 3E and F). The fluorescence intensity of the tumor region was 4.0-fold and 3.1-fold higher than that of the contralateral regions after the injection of DiI-labeled PEG-liposomes and DiI-labeled APRPG-liposomes, respectively.

### *3.3. Brain tumor imaging with positron-emitter-labeled liposomes by PET*

Finally, PEG-liposomes and APRPG-liposomes were labeled with the positron emitter [$^{18}$F]SteP2, by the SophT method, and injected into the glioma-bearing mice. As shown in Fig. 4, the positron emitter accumulated in the tumor region and imaged the tumor after injection in PEG-liposomes (Fig. 4, top panel) or APRPG-liposomes (Fig. 4, middle panel). Interestingly, the other regions of the brain showed a low background. On the contrary, [$^{18}$F]FDG imaged the whole brain, although the accumulation was higher in the tumor region (Fig. 4, bottom panel). BAS images (autoradiograms) shown in right panel confirmed the region of tumor. The tumor sizes of preparations varied to some extent in the present experiment, and the smallest tumor was revealed to be only about 1 mm in diameter. Interestingly, this small tumor was imaged by PET but was hardly detectable by CT when [$^{18}$F]SteP2-labeled APRPG-liposomes had been injected (Fig. 5).

The biodistribution of $^{18}$F at 1 h after the injection of [$^{18}$F]SteP2-labeled PEG-liposomes or [$^{18}$F]FDG is shown in Fig. 6. The liposome-bearing label was maintained in the bloodstream and highly accumulated in the spleen. This result is consistent with our previous study (Maeda et al., 2004). In the brain, $^{18}$F in the liposomes or as FDG significantly accumulated more in the tumor than in the normal tissues. In contrast to the distribution of $^{18}$F after injection of liposomes bearing it, $^{18}$F as FDG was cleared from the bloodstream quite fast and accumulated in the heart and normal region of brain.

## 4. Discussion

Since the usefulness of FDG-PET for the detection of brain tumors is controversial (Takeda et al., 2003; Chen, 2007), other PET imaging agents have been developed. In the present study, we aimed at imaging brain tumors not by the synthesis of molecules specifically taken up by tumor cells, but by use of DDS technology. Nanocarriers such as liposomes are well known to accumulate in solid tumors, especially in hypervascular tumors, due to the EPR effect (Maeda et al., 2000, 2009). In fact, liposomal radionuclides show effective tumor imaging (Oku et al., 1996; Geng et al., 2004; Elbayoumi and Torchilin, 2006). Moreover, liposome-based radionuclide delivery is not only useful for cancer imaging but also for cancer therapy when the carriers entrapping radiopharmaceuticals or other anticancer agents are used (Kostarelos and

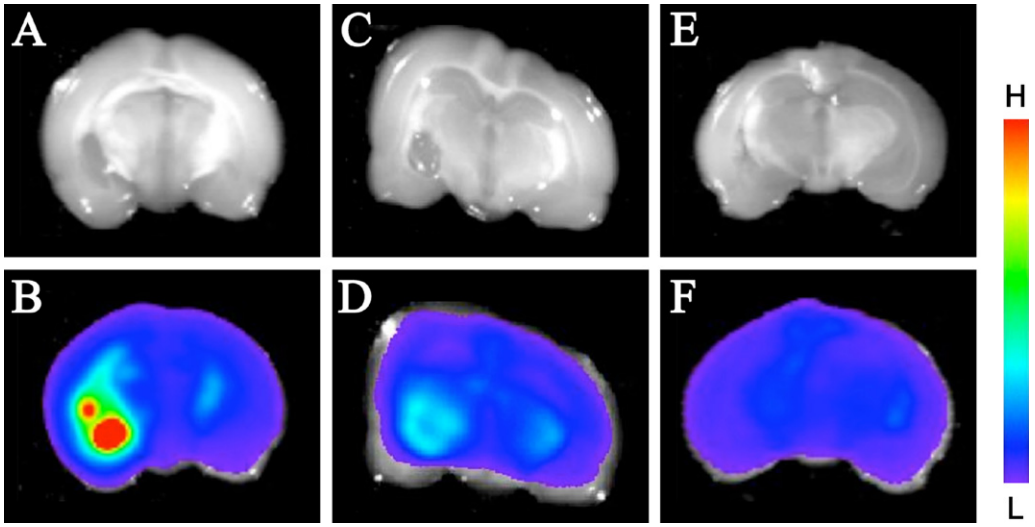


**Fig. 3.** *Ex vivo* imaging of liposomal distribution in rat brain bearing glioma. Rats were intravenously injected with DiI-labeled PEG-liposomes (A, B, E, and F) or APRPG-liposomes (C and D) at day 9 after implantation of C6 glioma cells (A–D) or medium alone (E and F) into the left midbrain. At 1 h after the injection, the brains were sliced into 2-mm sections, and the distribution of liposomes labeled with DiI was scanned with a fluorescence imaging system, IVIS (B, D, and F). Photos are also shown (A, C, and E). Two separate experiments gave similar results.

Emfietzoglou, 2000; Syme et al., 2003; Hamoudeh et al., 2008). Another advantage of carrier-based imaging is the active targeting by modifying carriers with some specific probes. We previously modified liposomes with angiogenic vessel-specific peptides and observed the efficient delivery of targeting liposomes to cancer by PET (Kondo et al., 2004; Maeda et al., 2006). Therefore, cancer imaging with DDS technology has various advantages including cancer treatment.

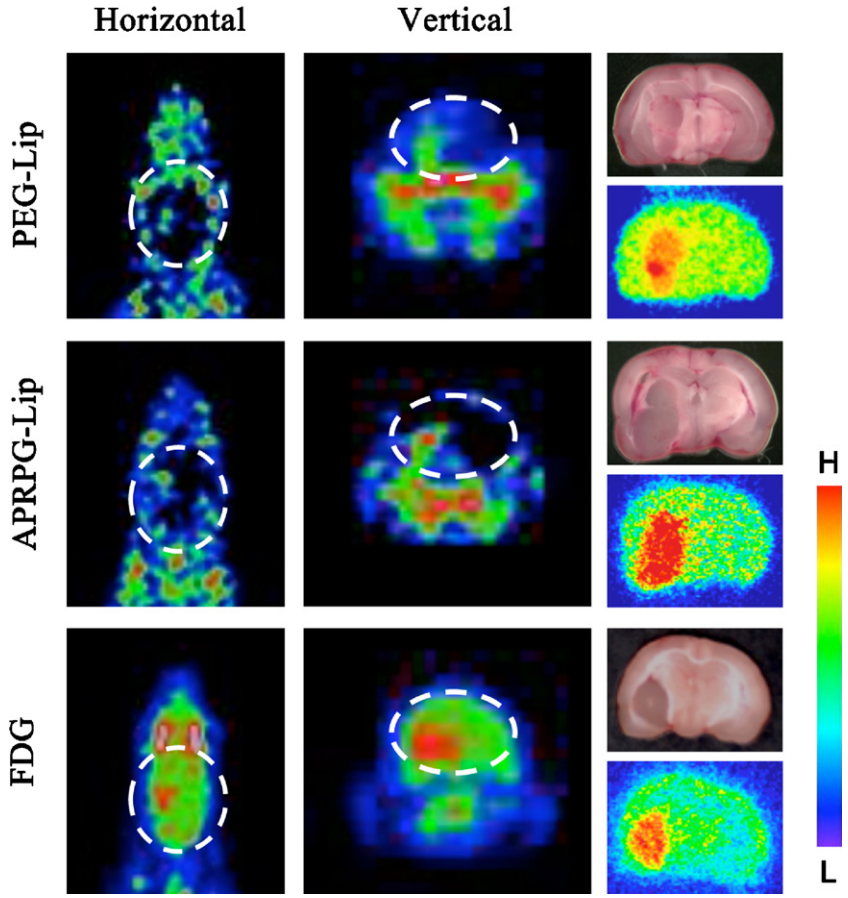


**Fig. 4.** PET imaging of brain tumor with [$^{18}$F]SteP2-liposomes and [$^{18}$F]-FDG. Rats were intravenously injected with 10 MBq of [$^{18}$F]SteP2-labeled PEG-liposomes (top panel), [$^{18}$F]SteP2-labeled APRPG-liposomes (middle panel) or [$^{18}$F]FDG (bottom panel) at day 11 after implantation of C6 glioma cells into the left midbrain. The biodistribution pattern of samples was determined by taking 1 frame/min for 1 h with the Clairvivo PET, and averaged data from 40 to 60 min are shown. Horizontal (left panel) and vertical (center panel) images are shown. After PET imaging, the brains were sliced into 2-mm sections, and the autoradiograms (right lower panels) were obtained with a bioimaging analyzer BAS 2000, and the pictures were taken (right upper panels). The ovals formed by the white dotted line show the estimated brain position.

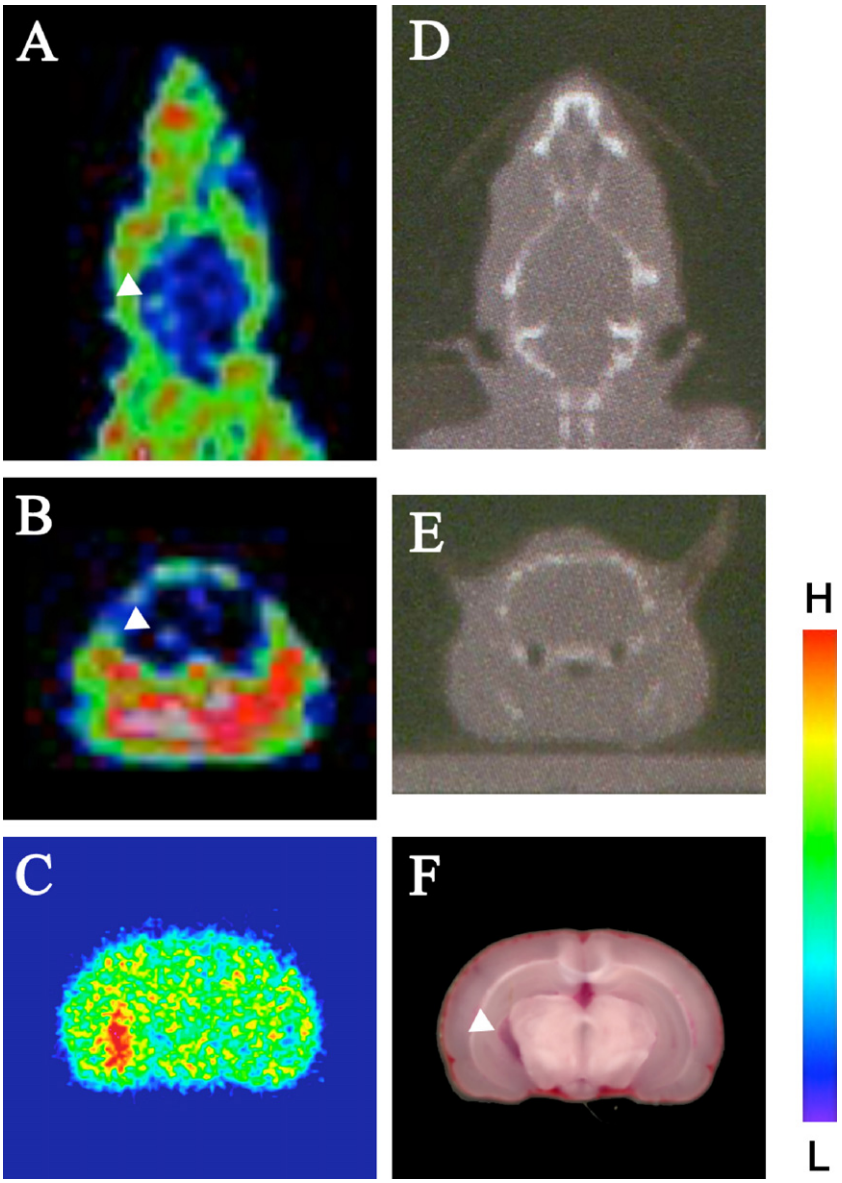


**Fig. 5.** PET imaging of small brain tumor with [$^{18}$F]SteP2-liposomes. PET imaging was performed as described in the legend of Fig. 4. Even the smallest tumor, 1-mm diameter, seen among the prepared model rats was imaged by PET. PET images (A and B) and CT images (D and E) of a rat brain are shown. Horizontal (A and D) and vertical (B and E) images are shown. (C) BAS image of a rat brain slice. (F) Photo of the brain slice. Arrowheads indicate the tumor.

It is well known that glioblastoma, the most prevalent brain cancer, is a hypervascular tumor due to angiogenesis (Verhoeff et al., 2009; Brastianos and Batchelor, 2009); and thus nanocarriers such as liposomes would be expected to accumulate in the brain cancer, since the permeability of tumor angiogenic vessels was higher than that of normal blood vessels. Moreover, brain blood vessels especially protect from the penetration of some molecules due to the BBB. Therefore, liposomes or other nanocarriers would be specifically accumulated into brain tumor region after circulating bloodstream, and be useful for brain cancer imaging. For labeling nanocarriers quite conveniently with PET probes, we previously synthesized a novel $^{18}$F-labeled amphiphilic compound known as 1-[$^{18}$F]fluoro-3,6-dioxatetracosane (Urakami et al., 2007). There are several methods for labeling liposomes, although radionuclides need to be incorporated during formulation of the liposomes in most of those methods. For example, to label liposomes with [$^{18}$F]FDG, [$^{18}$F]FDG was incorporated into liposomal aqueous phase during hydration step of liposomal lipids. In addition, the encapsulation efficiency of [$^{18}$F]FDG into the liposomes was very low. The advantage of the "solid-phase transition" (SophT) method is that it is applicable to preformed liposomes with quite high labeling efficiency. Moreover, [$^{18}$F]SteP2 in DSPC-based liposomes is stable in the presence of serum (Urakami et al., 2007). This universal method of liposomal modification can be used for various kinds of liposomes and lipidic nanoparticles and bring the enhanced detection of a target tissue.

Aim of the present study is to demonstrate the application of positron-labeled liposomes for brain tumor imaging by PET. We firstly examined the intratumoral distribution of fluorescence-labeled PEG- and APRPG-liposomes by fluorescence microscopy, and observed the accumulation of both DiI-labeled PEG-liposomes and APRPG-liposomes in the brain tumor region at 1 h after intravenous injection of the liposomes, although the intratumoral distribution of each liposome was different. We previously demonstrated that PEG-liposomes were accumulated around neovessels and fluorescence of DiI-labeled-APRPG-liposomes was colocalized with CD31 stain in colon 26 NL-17 solid tumor (Maeda et al., 2006). Therefore, the differential accumulation

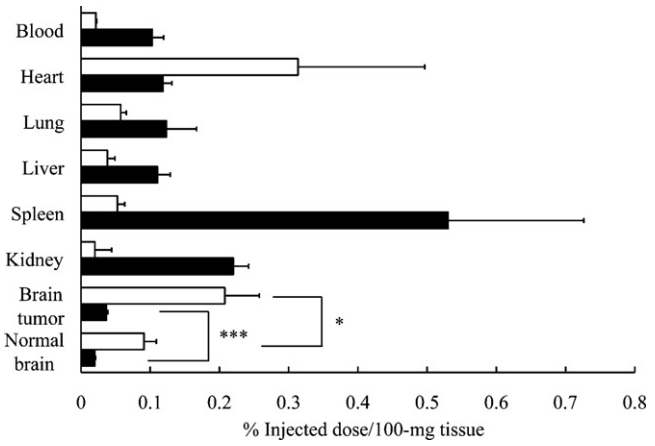


**Fig. 6.** Biodistribution of $^{18}$F after injection of [$^{18}$F]SteP2-labeled PEG-liposomes or [$^{18}$F]-FDG. Injection of [$^{18}$F]SteP2-labeled liposomes and [$^{18}$F]-FDG was performed as described in the legend of Fig. 4. At 1 h after the injection, blood was collected; and the selected organs were then excised for the determination of the radioactivity. Data are presented as the mean distribution of $^{18}$F after injection of [$^{18}$F]SteP2-labeled PEG-liposomes (closed bars, $n = 3$) or [$^{18}$F]FDG (open bars, $n = 4$). Significant differences between normal and tumor tissues are shown: $^{*}p < 0.05$, $^{***}p < 0.001$.

of PEG-liposomes and APRPG-liposomes observed in the tumor region, might be caused by the APRPG-modification of the latter liposomes.

In the present study HE-staining of normal brain tissue indicated that the capillaries were wrapped with astrocytes, whose arrangement may strengthen the BBB function (Standring, 2005). In contrast, astrocytes and nerve cells were not observed in the brain tumor tissues, and the capillaries directly faced the surrounding glioma cells: This might support the extravasation of PEG-liposomes into the tumor tissues. On the other hand, APRPG-liposomes might specifically accumulate in angiogenic vessels in brain tumor tissue. *Ex vivo* imaging of DiI with the *in vivo* fluorescence imaging system indicated the accumulation of both PEG-liposomes and APRPG-liposomes in the brain tumor was 3–4 fold higher than that in the surrounding normal brain tissue.

Our PET study indicated the accumulation of $^{18}$F-labeled liposomes and imaging of glioma in the tumor-bearing rat brain. The tumor images obtained with liposomes were clearer than those obtained with FDG-PET. In the case of [$^{18}$F]FDG imaging, the background level represented by imaging of normal brain region was high, since persistent demand for glucose to normal brain cells (Fig. 5). In contrast, brain tumor was specifically imaged by using [$^{18}$F]-labeled PEG- or APRPG-liposomes with quite low background. Additionally, those liposomes also can be used for the brain cancer therapy.

The efficiency for tumor imaging by both [$^{18}$F]SteP2-labeled PEG-liposomes and APRPG-liposomes was similar, although the intratumoral distribution was different between PEG-liposomes and APRPG-liposomes. These data are consistent with our previous results showing that the accumulation of PEG-liposomes and APRPG-liposomes in solid tumors was not much different (Maeda et al., 2004). Therefore, we conclude that [$^{18}$F]-labeled liposomes having either passive or active targeting characteristics are useful for brain tumor imaging: However, active targeting liposomes to tumor angiogenic endothelium would be more potent when these are used for both imaging and therapy. In the present study, it should be also noted that a tumor with a diameter of only 1 mm could be successfully imaged by using [$^{18}$F]SteP2-labeled liposomes.

## 5. Conclusions

In the present study, brain tumor imaging by a DDS nanocarrier, i.e., liposomes, was explored. Liposomes were $^{18}$F-labeled by the SophT method and injected intravenously into rats bearing a glioma-type brain tumor. Liposomes failed to accumulate in the normal surrounding brain tissue due to BBB protection and a brain tumor was specifically imaged with the liposomes via the different structure of brain tumor vessels. Since radiopharmaceutics or anticancer agents can be incorporated into DDS nanocarriers, these nanocarriers including liposomes should be useful for diagnosis and therapy of brain cancer.

## References

Asai, T., Shimizu, K., Kondo, M., Kuromi, K., Watanabe, K., Ogino, K., Taki, T., Shuto, S., Matsuda, A., Oku, N., 2002. Anti-neovascular therapy by liposomal DPP-CNDAC targeted to angiogenic vessels. FEBS Lett. 520, 167–170.

Brastianos, P.K., Batchelor, T.T., 2009. VEGF inhibitors in brain tumors. Clin. Adv. Hematol. Oncol. 768, 753–760.

Chen, W., 2007. Clinical applications of PET in brain tumors. J. Nucl. Med. 48, 1468–1481.

Elbayoumi, T.A., Torchilin, V.P., 2006. Enhanced accumulation of long-circulating liposomes modified with the nucleosome-specific monoclonal antibody 2C5 in various tumours in mice: gamma-imaging studies. Eur. J. Nucl. Med. Mol. Imaging 33, 1196–1205.

Floeth, F.W., Pauleit, D., Sabel, M., Stoffels, G., Reifenberger, G., Riemenschneider, M.J., Jansen, P., Coenen, H.H., Steiger, H.J., Langen, K.J., 2007. Prognostic value of *O*-(2-$^{18}$Ffluoroethyl)-L-tyrosine PET and MRI in low-grade glioma. J. Nucl. Med. 48, 519–527.

Gabizon, A.A., 2001. Pegylated liposomal doxorubicin: metamorphosis of an old drug into a new form of chemotherapy. Cancer Invest. 19, 424–436.

Geng, L., Osusky, K., Konjeti, S., Fu, A., Hallahan, D., 2004. Radiation-guided drug delivery to tumor blood vessels results in improved tumor growth delay. J. Control. Release 99, 369–381.

Hamoudeh, M., Kamleh, M.A., Diab, R., Fessi, H., 2008. Radionuclide delivery systems for nuclear imaging and radiotherapy of cancer. Adv. Drug Deliv. Rev. 60, 1329–1346.

Hatakeyama, T., Kawai, N., Nishiyama, Y., Yamamto, Y., Sasakawa, Y., Ichikawa, T., Tamiya, T., 2008. $^{11}$C-methionine (MET) and $^{18}$F-fluorothymidine (FLT) PET in patients with newly diagnosed glioma. Eur. J. Nucl. Med. Mol. Imaging 35, 2009–2017.

Heiss, P., Mayer, S., Herz, M., Wester, H.J., Schwaiger, M., Senekowitsch-Schmidtke, R., 1999. Investigation of transport mechanism and uptake kinetics of *O*-(2-[$^{18}$F]fluoroethyl)-L-tyrosine in vitro and in vivo. J. Nucl. Med. 40, 1367–1673.

Ishiwata, K., Kawamura, K., Wang, W.F., Furumoto, S., Kubota, K., Pascali, C., Bogni, A., Iwata, R., 2004. Evaluation of *O*-[$^{11}$C]methyl-L-tyrosine and *O*-[$^{18}$F]fluoromethyl-L-tyrosine as tumor imaging tracers by PET. Nucl. Med. Biol. 31, 191–198.

Jager, P.L., Vaalburg, W., Pruim, J., de Vries, E.G., Langen, K.J., Piers, D.A., 2001. Radiolabeled amino acids: basic aspects and clinical applications in oncology. J. Nucl. Med. 42, 432–445.

Kato, T., Shinoda, J., Nakayama, N., Miwa, K., Okumura, A., Yano, H., Yoshimura, S., Maruyama, T., Muragaki, Y., Iwama, T., 2008. Metabolic assessment of gliomas using $^{11}$C-methionine, [$^{18}$F] fluorodeoxyglucose, and $^{11}$C-choline positron-emission tomography. AJNR Am. J. Neuroradiol. 29, 1176–1182.

Kondo, M., Asai, T., Katanasaka, Y., Sadzuka, Y., Tsukada, H., Ogino, K., Taki, T., Baba, K., Oku, N., 2004. Anti-neovascular therapy by liposomal drug targeted to membrane type-1 matrix metalloproteinase. Int. J. Cancer 108, 301–306.

Kostarelos, K., Emfietzoglou, D., 2000. Tissue dosimetry of liposome–radionuclide complexes for internal radiotherapy: toward liposome-targeted therapeutic radiopharmaceuticals. Anticancer Res. 20, 3339–3345.

Langen, K.J., Hamacher, K., Weckesser, M., Floeth, F., Stoffels, G., Bauer, D., Coenen, H.H., Pauleit, D., 2006. *O*-(2-[$^{18}$F]fluoroethyl)-L-tyrosine: uptake mechanisms and clinical applications. Nucl. Med. Biol. 33, 287–294.

Maeda, H., Wu, J., Saw, T., Matsumura, Y., Hori, K., 2000. Tumor vascular permeability and the EPR effect in macromolecular therapeutics: a review. J. Control. Release 65, 271–284.

Maeda, H., Bharate, G.Y., Daruwalla, J., 2009. Polymeric drugs for efficient tumor-targeted drug delivery based on EPR-effect. Eur. J. Pharm. Biopharm. 71, 409–419.

Maeda, N., Takeuchi, Y., Takada, M., Sadzuka, Y., Namba, Y., Oku, N., 2004. Anti-neovascular therapy by use of tumor neovasculature-targeted long-circulating liposome. J. Control. Release 100, 41–52.

Maeda, N., Miyazawa, S., Shimizu, K., Asai, T., Yonezawa, S., Kitazawa, S., Namba, Y., Tsukada, H., Oku, N., 2006. Enhancement of anticancer activity in antineovascular therapy is based on the intratumoral distribution of the active targeting carrier for anticancer drugs. Biol. Pharm. Bull. 29, 1936–1940.

Mehrkens, J.H., Pöpperl, G., Rachinger, W., Herms, J., Seelos, K., Tatsch, K., Tonn, J.C., Kreth, F.W., 2008. The positive predictive value of *O*-(2-[$^{18}$F]fluoroethyl)-

L-tyrosine (FET) PET in the diagnosis of a glioma recurrence after multimodal treatment. J. Neurooncol. 88, 27–35.
Nakamoto, Y., Togashi, K., Kaneta, T., Fukuda, H., Nakajima, K., Kitajima, K., Murakami, K., Fujii, H., Satake, M., Tateishi, U., Kubota, K., Senda, M., 2009. Clinical value of whole-body FDG-PET for recurrent gastric cancer: a multicenter study. Jpn. J. Clin. Oncol. 39, 297–302.
Nojiri, T., Nariai, T., Aoyagi, M., Senda, M., Ishii, K., Ishiwata, K., Ohno, K., 2009. Contributions of biological tumor parameters to the incorporation rate of L-[methyl-$^{11}$C] methionine into astrocytomas and oligodendrogliomas. J. Neurooncol. 93, 233–241.
Oku, N., Tokudome, Y., Tsukada, H., Kosugi, T., Namba, Y., Okada, S., 1996. In vivo trafficking of long-circulating liposomes in tumour-bearing mice determined by positron emission tomography. Biopharm. Drug Dispos. 17, 435–441.
Oku, N., Asai, T., Watanabe, K., Kuromi, K., Nagatsuka, M., Kurohane, K., Kikkawa, H., Ogino, K., Tanaka, M., Ishikawa, D., Tsukada, H., Momose, M., Nakayama, J., Taki, T., 2002. Anti-neovascular therapy using novel peptides homing to angiogenic vessels. Oncogene 21, 2662–2669.
Pauleit, D., Stoffels, G., Bachofner, A., Floeth, F.W., Sabel, M., Herzog, H., Tellmann, L., Jansen, P., Reifenberger, G., Hamacher, K., Coenen, H.H., Langen, K.J., 2009. Comparison of $^{18}$F-FET and $^{18}$F-FDG PET in brain tumors. Nucl. Med. Biol. 36, 779–787.
Sakakibara, T., Chen, F.A., Kida, H., Kunieda, K., Cuenca, R.E., Martin, F.J., Bankert, R.B., 1996. Doxorubicin encapsulated in sterically stabilized liposomes is superior to free drug or drug-containing conventional liposomes at suppressing growth and metastases of human lung tumor xenografts. Cancer Res. 56, 3743–3746.
Scott, A.M., Gunawardana, D.H., Bartholomeusz, D., Ramshaw, J.E., Lin, P., 2008. PET changes management and improves prognostic stratification in patients with head and neck cancer: results of a multicenter prospective study. J. Nucl. Med. 49, 1593–1600.
Standring, S., 2005. GRAY'S Anatomy, 39th ed. Elsevier, Edinburgh, pp. 51–52.
Syme, A.M., McQuarrie, S.A., Middleton, J.W., Fallone, B.G., 2003. Dosimetric model for intraperitoneal targeted liposomal radioimmunotherapy of ovarian cancer micrometastases. Phys. Med. Biol. 48, 1305–1320.
Takeda, A., Tamano, H., Oku, N., 2003. Alteration of zinc concentrations in the brain implanted with C6 glioma. Brain Res. 965, 170–173.
Tang, G., Wang, M., Tang, X., Luo, L., Gan, M., 2003. Synthesis and evaluation of O-(3-[18F]fluoropropyl)-L-tyrosine as an oncologic PET tracer. Nucl. Med. Biol. 30, 733–739.
Tian, M., Zhang, H., Oriuchi, N., Higuchi, T., Endo, K., 2004. Comparison of $^{11}$C-choline PET and FDG PET for the differential diagnosis of malignant tumors. Eur. J. Nucl. Med. Mol. Imaging 31, 1064–1172.
Ullrich, R.T., Kracht, L., Brunn, A., Herholz, K., Frommolt, P., Miletic, H., Deckert, M., Heiss, W.D., Jacobs, A.H., 2009. Methyl-L-$^{11}$C-methionine PET as a diagnostic marker for malignant progression in patients with glioma. J. Nucl. Med. 50, 1962–1968.
Urakami, T., Akai, S., Katayama, Y., Harada, N., Tsukada, H., Oku, N., 2007. Novel amphiphilic probes for [$^{18}$F]-radiolabeling preformed liposomes and determination of liposomal trafficking by positron emission tomography. J. Med. Chem. 50, 6454–6457.
Urakami, T., Sakai, K., Asai, T., Fukumoto, D., Tsukada, H., Oku, N., 2009. Evaluation of *O*-[$^{18}$F]fluoromethyl-D-tyrosine as a radiotracer for tumor imaging with positron emission tomography. Nucl. Med. Biol. 36, 295–303.
Verhoeff, J.J., Stalpers, L.J., Claes, A., Hovinga, K.E., Musters, G.D., Vandertop, W.P., Richel, D.J., Leenders, W.P., van Furth, W.R., 2009. Tumour control by whole brain irradiation of anti-VEGF-treated mice bearing intracerebral glioma. Eur. J. Cancer 45, 3074–3080.
Wen, P.Y., Kesari, S., 2008. Malignant gliomas in adults. N. Engl. J. Med. 359, 492–507.
Yamamoto, Y., Nishiyama, Y., Kimura, N., Kameyama, R., Kawai, N., Hatakeyama, T., Kaji, M., Ohkawa, M., 2008. $^{11}$C-acetate PET in the evaluation of brain glioma: comparison with $^{11}$C-methionine and $^{18}$F-FDG-PET. Mol. Imaging Biol. 10, 281–287.